X-ray transitions in Br XXIV–XXVIII

J. F. Seely,* T. W. Phillips, R. S. Walling, J. Bailey, R. E. Stewart, and J. H. Scofield
University of California, Lawrence Livermore National Laboratory, Livermore, California 94550
(Received 19 February 1986)

Transitions in the wavelength region 4.9–8.1 Å from Br XXIV, XXV, XXVI, XXVII, and XXVIII have been identified in spectra from laser-produced plasmas. The identifications were made using *ab initio* calculations of wavelengths and oscillator strengths. Spatially resolved spectra were recorded for laser irradiation intensities from 3×10^{13} to 4×10^{14} W/cm^2. The dependence of the spectral lines on the distance from the target and on the irradiation intensity was very useful in distinguishing the transitions from different ionization stages.

I. INTRODUCTION

The demonstration of gain[1,2] on transitions in Ne-like selenium and yttrium has stimulated interest in the x-ray and extreme-ultraviolet spectroscopy of Ne-like ions. Gain was observed on transitions between the $2p^5 3s\,(J=1)$ and $2p^5 3p\,(J=2)$ levels, whereas computational modeling had predicted that the transition from the $2p^5 3p\,(J=0)$ level should have the highest gain. The improvement of these models may require the inclusion of processes other than electron collisional transitions from the ground state of a Ne-like ion.[3,4] This will require a knowledge of the densities and atomic rates from other charge states.

In this paper, we report the identification of x-ray transitions in the Mg-like through O-like ionization stages of bromine (Br XXIV, XXV, XXVI, XXVII, and XXVIII). Transitions in Ne-like Br XXVI have previously been observed by Burkhalter *et al.*,[5] Boiko *et al.*,[6] Hutcheon *et al.*,[7] and Gordon *et al.*[8] Burkhalter *et al.*[5] also identified several Na-like and Mg-like transitions that are satellites of the Ne-like transitions. Gordon and co-workers analyzed the Na-like spectra of bromine[8] and higher Z elements.[9] Transitions in F-like[7,8] and O-like[8] bromine have also been identified. The present work greatly expands the number of identified transitions in Br XXIV, XXV, XXVII, and XXVIII.

The plasma was produced from a laser-irradiated microdot of NaBr and NaCl, and the spectra were recorded by a spatially resolving crystal spectrometer. It was found that the Ne-like transitions diminished gradually as a function of distance from the target, and the Na-like transitions diminished very rapidly. The intensity of the laser was varied from 3×10^{13} to 4×10^{14} W/cm^2, and it was found that the Na-like and Ne-like transitions were dominant in the low-irradiation shots and that the Ne-like, F-like, and O-like transitions were dominant in the high-irradiation shots. The dependence of the spectral lines on the distance from the target and on the irradiation intensity was very useful in distinguishing the transitions from different ionization stages. A number of misidentifications in previous work have been corrected.

The transitions identified using *ab initio* calculations of the wavelengths and relative oscillator strengths (gf values) are discussed below and summarized in Tables I–VI. The measured and calculated wavelengths typically agreed to within a few mÅ. For isolated transitions that are collisionally excited from the ground state of a given ionization stage, the observed relative intensities and the calculated gf values were in good qualitative agreement. A more detailed study of the Ne-like intensities has been reported elsewhere.[10]

II. EXPERIMENTAL CONDITIONS

The experimental conditions have been discussed by Bailey *et al.*[10] The plasma was produced using the microdot technique.[11,12] A dot of target material composed of 10% NaBr, 90% NaCl, and a trace of Al was deposited onto a thick Mylar substrate. The diameter of the dot was 25 μm. The target was irradiated by the Phoenix laser beam ($\lambda=0.53$ μm) focused to a diameter of 100 μm and with a pulse duration of 800 psec. The plasma expanding from the microdot was confined to a column by the surrounding carbon plasma. The expansion of the microdot plasma was essentially one dimensional with a small transverse size, and this small size resulted in low opacity and narrow line profiles (typically 3 mÅ).

The spectra were recorded using a flat crystal spectrometer positioned to view the plasma at an angle of 5° to the target surface. Spatial resolution was provided by a slit parallel to the target surface and 30 μm in width. The crystal was Pentaerythritol (PET), and the resolving power of the instrument was $\lambda/\Delta\lambda=2500$. Single-shot spectra were recorded on Kodak Direct Exposure film.

III. WAVELENGTH MEASUREMENTS

The spectra produced using irradiation intensities of 3×10^{13} and 1×10^{14} W/cm^2 are shown in Fig. 1. The Na-like and Ne-like bromine transitions are intense in the low-irradiation (3×10^{13} W/cm^2) spectrum, and the high-irradiation (1×10^{14} W/cm^2) spectrum contains intense transitions from Ne-like, F-like, and O-like bromine. The Al XII $1s^2\,{}^1S_0-1s2p\,{}^1P_1$ transitions at 7.7575 Å is present on both spectra, and the Cl XVI $1s^2\,{}^1S_0-1s2p\,{}^1P_1$ transition (4.4445 Å) and dielectronic satellites appear on the

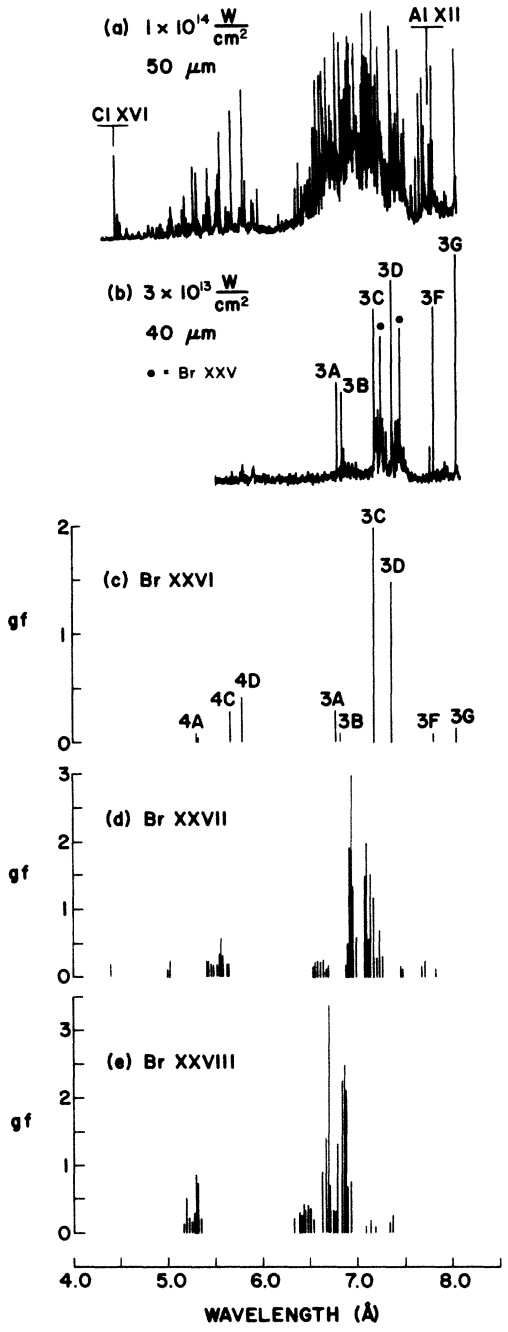

FIG. 1. (a) The bromine spectrum produced at an irradiation intensity of 1×10^{14} W/cm^2 and at a distance of 50 μm from the target and (b) the spectrum produced at 3×10^{13} W/cm^2 and 40 μm from the target. The gf values of some of the stronger transitions in Br XXVI, XXVII, and XXVIII are indicated in (c), (d), and (e), respectively.

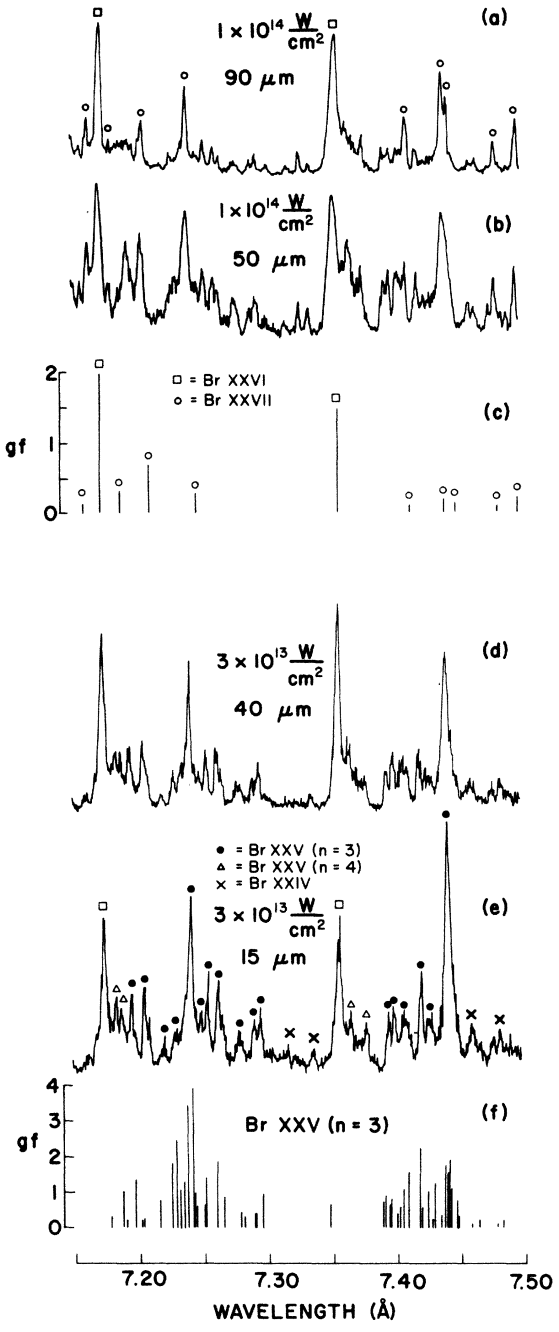

FIG. 2. The bromine spectra showing the Ne-like $3C$ and $3D$ transitions and the Na-like and Mg-like satellites at the indicated laser irradiation intensities and distances from the target are shown in (a), (b), (d), and (e). The gf values of transitions in Br XXV–XXVII are shown below the spectra in (c) and (f).

high-irradiation spectrum. The Al XII and Cl XVI resonance transitions were used as primary wavelength references, and we have adopted the wavelengths of Safronova.[13]

The wavelength scale for the high-irradiation spectrum, on which both the Al XII and Cl XVI reference lines appear, was established using these two reference lines and the geometry of the instrument. The wavelengths of the Ne-like transitions measured using this scale agree with the measurements of Hutcheon *et al.*[7] to within a few mÅ. The measurements of Gordon *et al.*[8] and of Boiko *et al.*[6] are systematically lower by up to 18 and 24 mÅ, respectively. The wavelengths on the low-irradiation spectrum were measured using the Ne-like transitions that

were measured in the high-irradiation spectrum as secondary references. The precision of the wavelengths, measured with respect to the Ne-like transitions, is estimated to be 2 mÅ. The accuracy of the absolute wavelengths depends on the accuracy of the wavelength scale of the high-irradiation spectrum, and this scale is believed to be accurate to 10 mÅ.

IV. LINE CALCULATION AND IDENTIFICATION

Identification of the lines in these spectra was accomplished by comparing the observed wavelengths and intensity patterns with those calculated for each of the ion stages expected in the plasma. *Ab initio* wavelengths and oscillator strengths were calculated using a relativistic atomic structure program written by one of us.[14] For each calculation, self-consistent Dirac-Fock orbitals were determined from an average-configuration potential including exchange. These single-particle orbitals were used to form states of total angular momentum J in jj coupling which were then used in the diagonalization for the eigenstates. For all ionization stages, we performed multiconfiguration diagonalizations. We used the length form of the dipole matrix operator for the oscillator strengths and have included a correction for the Breit interaction in our wavelengths. The amount of configuration interaction (CI) varied considerably for each ionization sequence. In each case we included those configurations which would cause significant mixtures with the configurations involved in our identifications. For highly charged ions, this implies at least the mixing of all configurations within the same spectroscopic complex. However, for Br XXIV transitions and the Br XXV transitions involving an $n=4$ spectator electron, we only included those configurations which have a hole in the $2p$ subshell. In addition, for any transitions involving an electron in a shell above $n=4$, we combined more approximate CI calculations with wavelength extrapolations from calculations for transitions from lower shells.

Our identifications are summarized in Tables I–VI and discussed by charge state below. The labels for the transitions in Tables II–VI correspond to the dominant jj-basis state component in each of the levels for the transitions. These components are labeled with respect to the vacancies in the $n=2$ shell and the occupancies in shells with $n \geq 3$. We have for simplicity suppressed the intermediate quantum numbers for all levels except those in Br XXVI. For these charge states, many levels are likely to have significant mixtures of several basis states; thus a complete description of these states would be unnecessarily complicated. For the transitions in Br XXVI (Table I), we retain the notation of Burkhalter *et al.*,[5] although these levels also may contain mixtures.

A. Ne-like transitions

The wavelengths and intensities of the Ne-like transitions, measured on the high-irradiation spectrum, are listed in Table I. The wavelengths are compared with the calculated wavelengths and with the previously measured wavelengths.[6–8] The presently measured wavelengths agree with the measurements of Hutcheon *et al.*[7] to within a standard deviation of 3 mÅ and are significantly larger than the measurements of Gordon *et al.*[8] and Boiko *et al.*[6] The profiles of the strongest $n=3$ transitions ($3C$, $3D$, $3F$, and $3G$) are distorted near the target, possibly by opacity.

A line at 7.44 Å has previously[5–7] been identified as the Ne-like $3E$ transition ($gf=0.007$). As shown in Fig. 2, the intensity of the 7.44-Å line in the low-irradiation spectrum is greater than the $3D$ transition ($gf=1.482$) near the target and diminishes rapidly away from the tar-

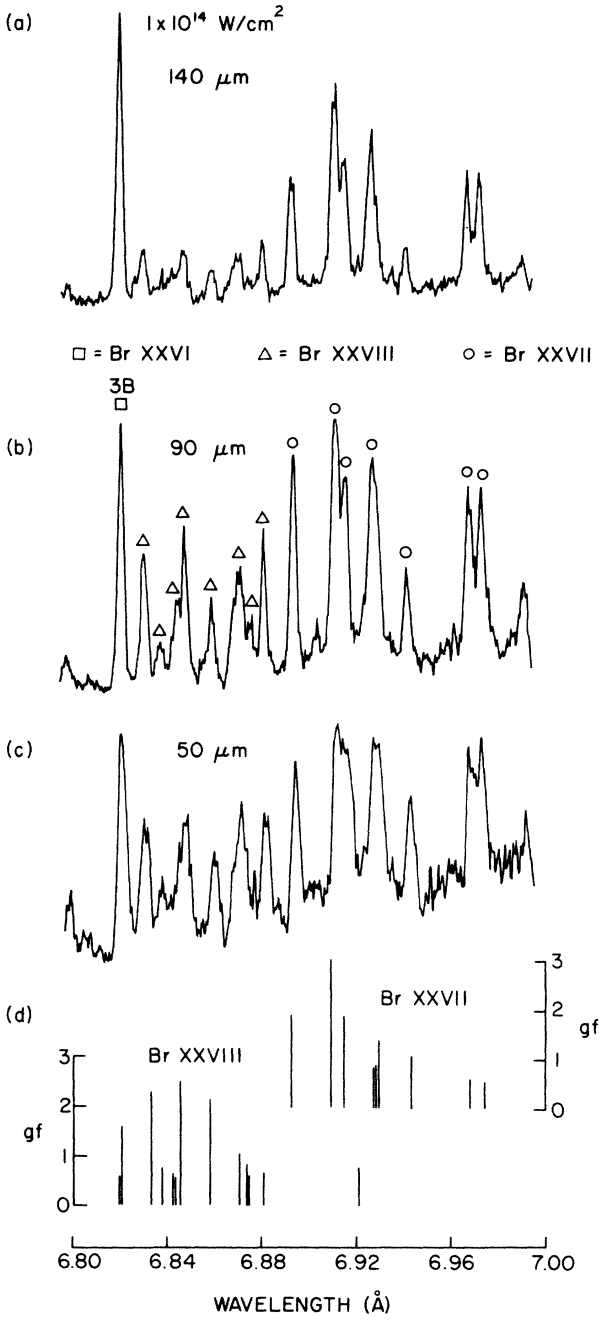

FIG. 3. The bromine spectrum from 6.8 to 7.0 Å and at distances of (a) 140 μm, (b) 90 μm, and (c) 50 μm from the target. Transitions in Ne-like, F-like, and O-like bromine are identified. The calculated gf values are shown in (d).

TABLE I. Transitions in Ne-like Br XXVI.

Key	Transition[a]	Pres. Meas. λ (Å)	Relative Intensity	Pres. Calc. λ	Pres. Calc. gf	Prev. Measured λ^b	Prev. Measured λ^c	Prev. Measured λ^d
$3G$	$2s^22p^6-[2p^5(^2P_{3/2}),3s]_1$	8.033	10	8.033	0.130	8.034	8.030	8.029
$3F$	$-[2p^5(^2P_{1/2}),3s]_1$	7.795	9	7.795	0.084	7.798	7.790	7.792
$3E$	$-[2p^5(^2P_{3/2}),3d(^2D_{3/2})]_1$	7.440	e	7.441	0.007	7.442	7.436	7.439
$3D$	$-[2p^5(^2P_{3/2}),3d(^2D_{5/2})]_1$	7.356	12	7.351	1.482	7.358	7.351	7.352
$3C$	$-[2p^5(^2P_{1/2}),3d(^2D_{3/2})]_1$	7.173	13	7.167	1.983	7.172	7.169	7.166
$3B$	$-[2s2p^63p(^2P_{1/2})]_1$	6.826	10	6.812	0.082	6.824	6.815	6.818
$3A$	$-[2s2p^63p(^2P_{3/2})]_1$	6.776	11	6.762	0.292	6.772	6.765	6.768
$4G$	$-[2p^5(^2P_{3/2}),4s]_1$	5.944	2	5.934	0.020	5.940	5.928	5.920
$4F$	$-[2p^5(^2P_{1/2}),4s]_1$	5.810	2	5.800	0.032	5.807	5.793	5.886
$4D$	$-[2p^5(^2P_{3/2}),4d(^2D_{5/2})]_1$	5.787	10	5.779	0.424	5.784	5.771	5.778
$4C$	$-[2p^5(^2P_{1/2}),4d(^2D_{3/2})]_1$	5.667	8	5.658	0.295	5.663	5.649	5.658
$4B$	$-[2s2p^64p(^2P_{1/2})]_1$	5.307	e	5.309	0.031		5.305	
$4A$	$-[2s2p^64p(^2P_{3/2})]_1$	5.299	e	5.297	0.089	5.305	5.292	
$5D$	$-[2p^5(^2P_{3/2}),5d(^2D_{5/2})]_1$	5.266	5	5.269	0.17	5.264	5.251	5.261
$5C$	$-[2p^5(^2P_{1/2}),5d(^2D_{3/2})]_1$	5.162	3	5.162	0.10	5.161	5.148	5.160
$6D$	$-[2p^5(^2P_{3/2}),6d(^2D_{5/2})]_1$	5.022	1	5.023	0.09		5.005	5.024
$6C$	$-[2p^5(^2P_{1/2}),6d(^2D_{3/2})]_1$	4.927	1	4.926	0.05			4.931

[a]The designation of the upper level includes the intermediate quantum numbers in parentheses.
[b]Hutcheon, Cooke, Key, Lewis, and Bromage (Ref. 7).
[c]Gordon, Hobby, and Peacock (Ref. 8).
[d]Boiko, Faenov, and Pikuz (Ref. 6).
[e]Blended with Br XXVIII transitions.

get. The 7.44-Å line in the low-irradiation spectrum is identified here as a Na-like transition at 7.441 Å with $gf=1.90$ (see Table II). In the high-irradiation spectrum shown in Fig. 2, the 7.44-Å feature diminishes gradually away from the target while the Na-like transitions diminish rapidly. It is also apparent in this spectrum that the 7.44-Å feature is a blend of more than one transition. In the high-irradiation spectrum near the target, the 7.44-Å feature is a blend of two F-like transitions at 7.439 and 7.443 Å (see Table V). However the $3E$ transition can be identified in the high-intensity spectra at distances far from the target where the other isolated F-like transitions are observed to disappear but the 7.44-Å feature persists. These new identifications illustrate the importance of having spectra with spatial resolution and taken at low- and high-irradiation intensities. The Ne-like $4A$ and $4B$ transitions are also blended with stronger O-like transitions.

A line at 5.305 Å was identified by Gordon *et al.*[8] as a blend of the $5B$ transition ($gf=0.014$). We observe a strong line at 5.307 Å in the high-irradiation spectrum, and this line diminishes with distance away from the target faster than the Ne-like transitions and in a manner similar to the O-like transitions. This line is identified here as the O-like transition with calculated wavelength 5.311 Å and $gf=0.75$ (see Table VI).

B. Na-like transitions

X-ray transitions in Na-like ions originate on upper levels with two $n=3$ electrons and a vacancy in the $n=2$ shell. The strongest transitions are of the type $3d$-$2p$ and $3p$-$2s$ and appear as satellites on the long-wavelength sides of the Ne-like $3C$ and $3D$ transitions. Na-like transitions with more highly excited spectator electrons ($n>3$) appear on the wings of the $3C$ and $3D$ transitions and are in many cases blended with the Ne-like transitions.

The wavelength region near the Ne-like $3C$ and $3D$ transitions and the Na-like satellites are shown in Fig. 2. The calculated gf values are shown below the spectra. Several F-like transitions are prominent in the high-irradiation spectrum shown in Fig. 2(a) and are weak in the low-irradiation spectrum shown in Figs. 2(d) and 2(e). The Na-like transitions diminish with distance from the target much more rapidly than the F-like and Ne-like transitions.

The Na-like transitions with $n=3$ electrons are listed in Table II. The measured wavelengths are in good agreement with the calculated wavelengths shifted to longer wavelengths by 0.002 Å. Several of our identifications differ from those of Gordon *et al.*[8] shown in the last column in Table II.

The spectral features appearing on the long-wavelength wings of the Ne-like $3C$ and $3D$ lines (see Fig. 2) are blends of a large number of Na-like transitions with an $n=4$ spectator electron. The wavelengths of the four observed spectral features are listed in Table III along with the calculated wavelengths and gf values.

C. Mg-like transitions

Listed in Table IV are the calculated wavelengths and gf values for the x-ray transitions that terminate on the

TABLE II. Transitions in Na-like Br XXV with $n=3$ excited levels.

Key	Transition[a]	Pres. Meas. λ (Å)	Relative Intensity	Pres. Calc. λ[b]	*gf*	Prev. Meas. λ[c]
1	$(3p_{3/2})-(2s_{1/2},3p_{3/2},3p_{3/2})_{3/2}$	6.844	5	6.842	0.56	
2	$(3s_{1/2})-(2p_{1/2},3s_{1/2},3d_{5/2})_{3/2}$	7.195	6	7.189	1.07	7.200
3	$(3p_{3/2})-(2p_{1/2},3p_{3/2},3d_{3/2})_{5/2}$	7.204	7	7.198	1.37	7.188
4	$(3d_{3/2})-(2p_{1/2},3d_{3/2},3d_{5/2})_{3/2}$			7.218	0.82	
5	$(3d_{5/2})-(2p_{1/2},3d_{3/2},3d_{5/2})_{3/2}$			7.226	1.81	
6	$(3d_{3/2})-(2p_{1/2},3d_{3/2},3d_{3/2})_{3/2}$	7.229	3	7.230	2.49	
7	$(3p_{3/2})-(2p_{1/2},3p_{3/2},3d_{3/2})_{1/2}$			7.233	1.11	
8	$(3p_{1/2})-(2p_{1/2},3p_{1/2},3d_{3/2})_{1/2}$			7.233	0.93	
9	$(3s_{1/2})-(2p_{1/2},3s_{1/2},3d_{3/2})_{1/2}$			7.236	1.31	
10	$(3p_{3/2})-(2p_{1/2},3p_{3/2},3d_{3/2})_{3/2}$			7.238	1.60	
11	$(3d_{5/2})-(2p_{1/2},3d_{3/2},3d_{5/2})_{7/2}$			7.238	3.42	7.232
12	$(3d_{5/2})-(2p_{1/2},3d_{3/2},3d_{3/2})_{3/2}$			7.239	0.65	
13	$(3d_{5/2})-(2p_{1/2},3d_{3/2},3d_{5/2})_{5/2}$	7.240	13	7.243	3.93	7.246
14	$(3p_{3/2})-(2p_{1/2},3p_{1/2},3d_{5/2})_{5/2}$			7.244	0.96	
15	$(3d_{3/2})-(2p_{1/2},3d_{3/2},3d_{3/2})_{1/2}$			7.246	0.65	
16	$(3p_{3/2})-(2p_{1/2},3p_{1/2},3d_{3/2})_{3/2}$			7.252	0.66	
17	$(3s_{1/2})-(2p_{1/2},3s_{1/2},3d_{3/2})_{3/2}$	7.254	7	7.253	1.44	
18	$(3p_{1/2})-(2p_{1/2},3p_{1/2},3d_{3/2})_{3/2}$	7.262	7	7.262	1.88	7.254
19	$(3p_{3/2})-(2p_{1/2},3p_{3/2},3d_{5/2})_{5/2}$	7.266	1	7.268	0.88	
20	$(3p_{3/2})-(2p_{1/2},3p_{3/2},3d_{5/2})_{5/2}$	7.279	2	7.280	0.44	
21	$(3d_{5/2})-(2p_{1/2},3d_{3/2},3d_{5/2})_{5/2}$	7.290	3	7.291	0.42	
22	$(3d_{5/2})-(2p_{1/2},3d_{5/2},3d_{5/2})_{7/2}$			7.292	0.41	
23	$(3d_{3/2})-(2p_{1/2},3d_{3/2},3d_{3/2})_{5/2}$	7.295	4	7.298	0.96	7.285
24	$(3p_{1/2})-(2p_{3/2},3p_{3/2},3d_{3/2})_{3/2}$			7.349	0.69	
25	$(3d_{5/2})-(2p_{3/2},3d_{5/2},3d_{5/2})_{3/2}$			7.391	0.75	7.391
26	$(3s_{1/2})-(2p_{3/2},3s_{1/2},3d_{5/2})_{3/2}$	7.395	4	7.393	0.91	
27	$(3p_{3/2})-(2p_{3/2},3p_{3/2},3d_{5/2})_{5/2}$			7.396	0.69	
28	$(3p_{3/2})-(2p_{3/2},3p_{3/2},3d_{5/2})_{1/2}$	7.399	5	7.397	0.81	
29	$(3s_{1/2})-(2p_{3/2},3s_{1/2},3d_{5/2})_{1/2}$			7.407	0.61	
30	$(3d_{3/2})-(2p_{3/2},3d_{3/2},3d_{5/2})_{1/2}$			7.410	1.11	
31	$(3d_{3/2})-(2p_{3/2},3d_{3/2},3d_{5/2})_{5/2}$	7.407	5	7.410	1.59	7.403
32	$(3d_{5/2})-(2p_{3/2},3d_{3/2},3d_{5/2})_{5/2}$	7.420	7	7.419	2.22	7.413
33	$(3p_{1/2})-(2p_{3/2},3p_{1/2},3d_{5/2})_{1/2}$			7.421	0.57	
34	$(3d_{5/2})-(2p_{3/2},3d_{5/2},3d_{5/2})_{3/2}$			7.425	1.03	
35	$(3p_{3/2})-(2p_{3/2},3p_{3/2},3d_{5/2})_{3/2}$	7.427	2	7.431	1.27	
36	$(3d_{3/2})-(2p_{3/2},3d_{3/2},3d_{5/2})_{5/2}$			7.439	1.77	
37	$(3p_{3/2})-(2p_{3/2},3p_{3/2},3d_{5/2})_{5/2}$			7.441	1.55	
38	$(3s_{1/2})-(2p_{3/2},3s_{1/2},3d_{5/2})_{3/2}$			7.441	0.82	
39	$(3d_{5/2})-(2p_{3/2},3d_{5/2},3d_{5/2})_{7/2}$	7.441	14	7.442	1.90	7.436
40	$(3d_{3/2})-(2p_{3/2},3d_{3/2},3d_{5/2})_{3/2}$			7.443	1.12	
41	$(3d_{5/2})-(2p_{3/2},3d_{3/2},3d_{5/2})_{5/2}$			7.448	0.75	

[a]The designation is (lower level, upper level: hole state, excited state) *J*, where hole state is the missing $n=2$ electron, excited state is the list of $n=3$ electrons, and *J* is the total angular momentum.
[b]*Ab initio* calculations shifted to longer wavelengths by 0.002 Å.
[c]Gordon, Hobby, and Peacock (Ref. 8).

$2p^63s^2$ or $2p^63s3p$ levels of Mg-like Br XXIV. The upper levels of these transitions have one missing $2p$ electron. Many of these transitions are blended with stronger Na-like transitions. Four spectral lines are identified in the low-irradiation spectrum as Mg-like transitions, and all four of these lines are very weak. The 7.460-Å line is the same transition observed by Burkhalter *et al.*[5] in the elements Se and Zr and by Gordon *et al.*[9] in the elements Kr through Mo. Several transitions to the $2p^63p3d$ and $2p^63d^2$ levels have much higher *gf* values (up to $gf=5.5$), but these transitions are not present in the spectra. However, these transitions require the population of configurations involving two excited electrons and are thus expected to be weak.

D. F-like transitions

The F-like transitions are prominent in the high-irradiation spectrum, and the classification of these transitions is given in Table V. Also listed are the classifica-

TABLE III. Transitions in Na-like Br XXV with $n=4$ excited levels.

Key	Transition[a]	Meas. λ	Meas. Relative Intensity	Calc. λ[b]	Calc. gf
1	$(4f_{7/2})-(2p_{1/2},3d_{3/2},4f_{7/2})_{9/2}$			7.160	4.16
2	$(4f_{7/2})-(2p_{1/2},3d_{3/2},4f_{7/2})_{5/2}$			7.170	2.94
3	$(4f_{5/2})-(2p_{1/2},3d_{3/2},4f_{5/2})_{5/2}$			7.175	2.85
4	$(4f_{7/2})-(2p_{1/2},3d_{3/2},4f_{7/2})_{7/2}$			7.178	4.48
5	$(4d_{5/2})-(2p_{1/2},3d_{3/2},4d_{5/2})_{7/2}$			7.182	3.89
6	$(4p_{3/2})-(2p_{1/2},3d_{3/2},4p_{3/2})_{5/2}$	7.183	5	7.184	3.42
7	$(4p_{1/2})-(2p_{1/2},3d_{3/2},4p_{1/2})_{3/2}$			7.184	2.30
8	$(4d_{5/2})-(2p_{1/2},3d_{3/2},4d_{5/2})_{5/2}$			7.187	3.14
9	$(4f_{5/2})-(2p_{1/2},3d_{3/2},4f_{5/2})_{7/2}$	7.187	4	7.189	4.64
10	$(4p_{3/2})-(2p_{1/2},3d_{3/2},4p_{3/2})_{3/2}$			7.190	2.35
11	$(4d_{3/2})-(2p_{1/2},3d_{3/2},4d_{3/2})_{5/2}$			7.193	3.62
12	$(4f_{7/2})-(2p_{3/2},3d_{5/2},4f_{7/2})_{5/2}$			7.354	2.53
13	$(4f_{5/2})-(2p_{3/2},3d_{5/2},4f_{5/2})_{7/2}$			7.357	2.89
14	$(4f_{7/2})-(2p_{3/2},3d_{5/2},4f_{7/2})_{9/2}$			7.360	3.38
15	$(4f_{7/2})-(2p_{3/2},3d_{5/2},4f_{7/2})_{7/2}$	7.366	4	7.364	3.29
16	$(4f_{5/2})-(2p_{3/2},3d_{5/2},4f_{5/2})_{5/2}$			7.365	2.48
17	$(4p_{3/2})-(2p_{3/2},3d_{5/2},4p_{3/2})_{5/2}$			7.371	2.62
18	$(4d_{5/2})-(2p_{3/2},3d_{5/2},4d_{5/2})_{7/2}$	7.377	4	7.375	3.48

[a]The designation is (lower level, upper level: hole state, excited state) J, where hole state is the missing $n=2$ electron, excited state is the list of excited electrons, and J is the total angular momentum.
[b]*Ab initio* calculations shifted to longer wavelengths by 0.002 Å.

tions of Hutcheon *et al.*[7] and of Gordon *et al.*[8] In the cases where these authors assigned the same measured wavelength to more than one transition, we have assigned their measured wavelength to the transition with the largest gf value. When this is done, then our classifications are in substantial agreement with the classifications of Hutcheon *et al.*[7] and of Gordon *et al.*,[8] where comparisons can be made. The high resolving power of our instrument and the small source size resulting from the use of the microdot technique resulted in narrow linewidths and in the resolution of a number of blends in the earlier spectra.[7,8] The agreement with the calculated wavelengths is typically within 7 mÅ.

E. O-like transitions

The O-like transitions are also present in the high-irradiation spectrum. Figure 3 illustrates the spectral region from 6.8 to 7.0 Å, where F-like, O-like, and Ne-like transitions appear. The intensities of these spectral lines vary differently with distance from the target surface depending on ionization stage. This variation is useful in distinguishing the O-like from the F-like transitions. The measured wavelengths of the O-like transitions thus identified are listed in Table VI. Where comparisons can be made, our measurements are in satisfactory agreement with the results of Gordon *et al.*[8] With a few exceptions,

TABLE IV. Transitions in Mg-like Br XXIV.

Key	Transition[a]	Pres. Meas. λ	Pres. Meas. Relative Intensity	Pres. Calc. λ	Pres. Calc. gf	Prev. Meas. λ[b]
1	$(3s_{1/2},3s_{1/2})_0-(2p_{1/2},3s_{1/2},3s_{1/2},3d_{3/2})_1$	7.262	c	7.264	1.48	
2	$(3s_{1/2},3p_{3/2})_1-(2p_{1/2},3s_{1/2},3p_{3/2},3d_{3/2})_1$	7.266	c	7.267	1.34	
3	$(3s_{1/2},3p_{3/2})_2-(2p_{1/2},3s_{1/2},3p_{3/2},3d_{5/2})_3$	7.279	c	7.273	1.95	
4	$(3s_{1/2},3p_{3/2})_1-(2p_{1/2},3s_{1/2},3p_{3/2},3d_{3/2})_2$	7.290	c	7.282	1.60	
5	$(3s_{1/2},3p_{3/2})_2-(2p_{1/2},3s_{1/2},3p_{3/2},3d_{3/2})_1$	7.295	c	7.291	1.16	
6	$(3s_{1/2},3p_{3/2})_2-(2p_{1/2},3s_{1/2},3p_{3/2},3d_{3/2})_2$	7.316	1	7.308	1.44	
7	$(3s_{1/2},3p_{1/2})_0-(2p_{1/2},3s_{1/2},3p_{1/2},3d_{3/2})_1$	7.336	1	7.323	1.03	
8	$(3s_{1/2},3s_{1/2})_0-(2p_{3/2},3s_{1/2},3s_{1/2},3d_{5/2})_1$	7.460	1	7.455	0.97	7.46
9	$(3s_{1/2},3p_{3/2})_2-(2p_{3/2},3s_{1/2},3p_{3/2},3d_{5/2})_3$			7.474	1.12	
10	$(3s_{1/2},3p_{3/2})_1-(2p_{3/2},3s_{1/2},3p_{3/2},3d_{5/2})_2$	7.481	1	7.484	1.09	

[a]The designation is (lower level, upper level: hole state, excited state) J, where hole state is the missing $n=2$ electron, excited state is the list of $n=3$ electrons, and J is the total angular momentum.
[b]Extrapolated from the measurements of Gordon *et al.* (Ref. 9) for the elements Kr through Mo.
[c]Blended with Br XXV transitions.

TABLE V. Transitions in F-like Br XXVII.

Key	Transition[a]	Pres. Meas. λ	Relative Intensity	Pres. Calc. λ[b]	*gf*	Prev. Meas. λ[c]	λ[d]
1	$(2p_{1/2})-(2p_{1/2},2p_{3/2},5d_{5/2})_{1/2}$			5.017	0.12		
2	$(2p_{1/2})-(2p_{1/2},2p_{3/2},5d_{5/2})_{3/2}$	5.014	1	5.018	0.13		
3	$(2p_{3/2})-(2p_{3/2},2p_{3/2},5d_{5/2})_{5/2}$	5.033	2	5.037	0.26		
4	$(2p_{3/2})-(2p_{3/2},2p_{3/2},5d_{5/2})_{3/2}$			5.037	0.15		
5	$(2p_{3/2})-(2s_{1/2},2p_{3/2},4p_{3/2})_{5/2}$	5.111	1	5.114	0.08		
6	$(2p_{3/2})-(2s_{1/2},2p_{3/2},4p_{3/2})_{5/2}$			5.159	0.09		
7	$(2p_{3/2})-(2s_{1/2},2p_{3/2},4p_{3/2})_{3/2}$	5.155	2	5.160	0.10		
8	$(2p_{3/2})-(2s_{1/2},2p_{3/2},4p_{1/2})_{5/2}$	5.167	1	5.171	0.08		
9	$(2p_{1/2})-(2p_{1/2},2p_{1/2},4d_{3/2})_{3/2}$	5.401	2	5.408	0.26		5.400
10	$(2p_{3/2})-(2p_{1/2},2p_{3/2},4d_{5/2})_{3/2}$	5.407	1	5.414	0.08		5.412
11	$(2p_{3/2})-(2p_{1/2},2p_{3/2},4d_{3/2})_{5/2}$	5.416	4	5.420	0.26		5.429
12	$(2p_{3/2})-(2p_{1/2},2p_{3/2},4d_{3/2})_{3/2}$	5.426	1	5.422	0.24		
13	$(2p_{3/2})-(2p_{1/2},2p_{3/2},4d_{3/2})_{1/2}$			5.423	0.15		
14	$(2s_{1/2})-(2s_{1/2},2p_{1/2},4d_{3/2})_{1/2}$			5.434	0.20		
15	$(2s_{1/2})-(2s_{1/2},2p_{1/2},4d_{5/2})_{3/2}$			5.435	0.18		
16	$(2p_{3/2})-(2p_{1/2},2p_{3/2},4d_{3/2})_{5/2}$	5.445	2	5.452	0.21		5.493
17	$(2s_{1/2})-(2s_{1/2},2p_{1/2},4d_{3/2})_{3/2}$	5.500	1	5.512	0.15		5.507
18	$(2p_{3/2})-(2p_{3/2},2p_{3/2},4d_{5/2})_{5/2}$	5.510	2	5.516	0.20		
19	$(2p_{1/2})-(2p_{1/2},2p_{3/2},4d_{5/2})_{1/2}$			5.530	0.25		
20	$(2p_{1/2})-(2p_{1/2},2p_{3/2},4d_{5/2})_{3/2}$	5.526	4	5.531	0.36		
21	$(2p_{3/2})-(2p_{3/2},2p_{3/2},4d_{5/2})_{5/2}$	5.548	8	5.553	0.58		5.530
22	$(2p_{3/2})-(2p_{3/2},2p_{3/2},4d_{5/2})_{3/2}$	5.560	2	5.555	0.30		
23	$(2p_{1/2})-(2p_{1/2},2p_{3/2},4d_{5/2})_{3/2}$	5.564	2	5.565	0.17		
24	$(2s_{1/2})-(2s_{1/2},2p_{3/2},4d_{5/2})_{3/2}$			5.574	0.33		
25	$(2s_{1/2})-(2s_{1/2},2p_{3/2},4d_{5/2})_{1/2}$	5.609	1	5.622	0.21		
26	$(2s_{1/2})-(2s_{1/2},2p_{3/2},4d_{5/2})_{3/2}$	5.617	1	5.629	0.19		
27	$(2p_{3/2})-(2s_{1/2},2p_{1/2},3p_{3/2})_{5/2}$	6.374	4	6.368	0.07		6.359
28	$(2p_{1/2})-(2s_{1/2},2p_{1/2},3p_{3/2})_{3/2}$	6.527	6	6.521	0.16		6.512
29	$(2p_{1/2})-(2s_{1/2},2p_{1/2},3p_{3/2})_{1/2}$	6.542	6	6.536	0.16		6.531
30	$(2s_{1/2})-(2s_{1/2},2s_{1/2},3p_{2/3})_{3/2}$	6.547	5	6.537	0.23		
31	$(2p_{3/2})-(2s_{1/2},2p_{3/2},3p_{3/2})_{3/2}$			6.565	0.08		
32	$(2p_{3/2})-(2s_{1/2},2p_{3/2},3p_{3/2})_{5/2}$	6.566	5	6.568	0.25		6.556
33	$(2p_{1/2})-(2s_{1/2},2p_{1/2},3p_{1/2})_{3/2}$	6.569	10	6.573	0.17		6.567
34	$(2s_{1/2})-(2s_{1/2},2s_{1/2},3p_{1/2})_{1/2}$	6.579	5	6.579	0.11		
35	$(2p_{3/2})-(2s_{1/2},2p_{3/2},3p_{1/2})_{1/2}$	6.609	10	6.604	0.24		6.598
36	$(2p_{3/2})-(2s_{1/2},2p_{3/2},3p_{1/2})_{3/2}$			6.608	0.22		
37	$(2p_{3/2})-(2s_{1/2},2p_{3/2},3p_{3/2})_{5/2}$	6.635	7	6.634	0.27		6.624
38	$(2p_{1/2})-(2s_{1/2},2p_{1/2},3p_{3/2})_{3/2}$	6.639	5	6.638	0.13		
39	$(2p_{3/2})-(2s_{1/2},2p_{3/2},3p_{3/2})_{3/2}$	6.644	4	6.644	0.18		6.633
40	$(2p_{1/2})-(2s_{1/2},2p_{1/2},3p_{1/2})_{1/2}$	6.664	2	6.665	0.13		
41	$(2p_{3/2})-(2s_{1/2},2p_{3/2},3p_{1/2})_{5/2}$	6.688	e	6.687	0.18		6.674
42	$(2p_{3/2})-(2p_{1/2},2p_{3/2},3d_{5/2})_{1/2}$	6.876	e	6.878	0.19		
43	$(2p_{3/2})-(2p_{1/2},2p_{3/2},3d_{3/2})_{3/2}$	6.886	e	6.888	0.49		6.877
44	$(2p_{1/2})-(2p_{1/2},2p_{1/2},3d_{3/2})_{3/2}$	6.899	9	6.903	1.90		6.888
45	$(2p_{3/2})-(2p_{1/2},2p_{3/2},3d_{3/2})_{5/2}$	6.917	10	6.919	2.96	6.918	6.905
46	$(2p_{3/2})-(2p_{1/2},2p_{3/2},3d_{3/2})_{3/2}$	6.921	8	6.925	1.86		6.909
47	$(2s_{1/2})-(2s_{1/2},2p_{1/2},3d_{3/2})_{3/2}$			6.931	0.86		
48	$(2s_{1/2})-(2s_{1/2},2p_{1/2},3d_{3/2})_{1/2}$	6.932	9	6.932	1.36		
49	$(2p_{3/2})-(2p_{1/2},2p_{3/2},3d_{5/2})_{5/2}$			6.938	0.12		
50	$(2p_{3/2})-(2p_{1/2},2p_{3/2},3d_{3/2})_{1/2}$			6.938	0.86	6.931	6.925
51	$(2s_{1/2})-(2s_{1/2},2p_{1/2},3d_{5/2})_{3/2}$	6.947	5	6.946	1.05		
52	$(2p_{3/2})-(2p_{1/2},2p_{3/2},3d_{5/2})_{5/2}$	6.973	8	6.978	0.60	6.972	6.966
53	$(2p_{3/2})-(2p_{1/2},2p_{3/2},3d_{5/2})_{5/2}$	6.978	8	6.985	0.54	6.991	6.983
54	$(2s_{1/2})-(2s_{1/2},2p_{1/2},3d_{3/2})_{3/2}$	7.056	5	7.061	1.13		
55	$(2p_{1/2})-(2p_{1/2},2p_{3/2},3d_{5/2})_{1/2}$	7.066	8	7.068	1.48	7.063	7.057
56	$(2p_{1/2})-(2p_{1/2},2p_{3/2},3d_{3/2})_{3/2}$	7.078	10	7.079	1.98	7.077	7.071
57	$(2p_{3/2})-(2p_{3/2},2p_{3/2},3d_{5/2})_{5/2}$	7.092	7	7.087	1.07		
58	$(2p_{3/2})-(2p_{3/2},2p_{3/2},3d_{3/2})_{3/2}$	7.106	2	7.100	0.57	7.092	

TABLE V. (*Continued*).

Key	Transition[a]	Pres. Meas. λ	Relative Intensity	Pres. Calc. λ[b]	*gf*	Prev. Meas. λ[c]	λ[d]
59	$(2p_{1/2})-(2p_{1/2},2p_{3/2},3d_{3/2})_{3/2}$	7.114	4	7.118	0.32		
60	$(2p_{3/2})-(2p_{3/2},2p_{3/2},3d_{5/2})_{5/2}$	7.119	9	7.125	1.51	7.118	7.111
61	$(2p_{1/2})-(2p_{1/2},2p_{3/2},3d_{3/2})_{1/2}$			7.131	0.09		
62	$(2p_{3/2})-(2p_{3/2},2p_{3/2},3d_{5/2})_{3/2}$	7.132	7	7.140	0.71	7.132	7.124
63	$(2s_{1/2})-(2s_{1/2},2p_{3/2},3d_{5/2})_{3/2}$	7.149	6	7.155	1.21		
64	$(2p_{3/2})-(2p_{3/2},2p_{3/2},3d_{5/2})_{1/2}$	7.159	2	7.156	0.36	7.150	7.140
65	$(2p_{1/2})-(2p_{1/2},2p_{3/2},3d_{5/2})_{3/2}$	7.164	5	7.171	0.15		
66	$(2s_{1/2})-(2s_{1/2},2p_{3/2},3d_{3/2})_{3/2}$	7.181	1	7.191	0.08		
67	$(2s_{1/2})-(2s_{1/2},2p_{3/2},3d_{3/2})_{1/2}$	7.195	2	7.191	0.28		
68	$(2s_{1/2})-(2s_{1/2},2p_{3/2},3d_{5/2})_{1/2}$	7.206	4	7.213	0.72		
69	$(2s_{1/2})-(2s_{1/2},2p_{3/2},3d_{5/2})_{3/2}$	7.240	7	7.249	0.32		
70	$(2p_{1/2})-(2p_{3/2},2p_{3/2},3d_{5/2})_{3/2}$	7.337	1	7.345	0.02		
71	$(2p_{1/2})-(2p_{1/2},2p_{1/2},3s_{1/2})_{1/2}$	7.411	5	7.425	0.07		7.403
72	$(2p_{3/2})-(2p_{1/2},2p_{3/2},3s_{1/2})_{5/2}$	7.439	8	7.451	0.17		7.436
73	$(2s_{1/2})-(2s_{1/2},2p_{1/2},3s_{1/2})_{3/2}$	7.443	6	7.451	0.14		
74	$(2p_{3/2})-(2p_{1/2},2p_{3/2},3s_{1/2})_{1/2}$	7.480	3	7.493	0.05		7.473
75	$(2p_{3/2})-(2p_{1/2},2p_{3/2},3s_{1/2})_{3/2}$	7.496	5	7.510	0.06		7.488
76	$(2s_{1/2})-(2s_{1/2},2p_{1/2},3s_{1/2})_{1/2}$	7.572	1	7.585	0.05		
77	$(2p_{3/2})-(2p_{3/2},2p_{3/2},3s_{1/2})_{1/2}$	7.615	2	7.631	0.05	7.617	7.608
78	$(2p_{1/2})-(2p_{1/2},2p_{3/2},3s_{1/2})_{3/2}$	7.655	7	7.668	0.16	7.657	7.651
79	$(2p_{3/2})-(2p_{3/2},2p_{3/2},3s_{1/2})_{3/2}$	7.690	8	7.705	0.24	7.692	7.685
80	$(2s_{1/2})-(2s_{1/2},2p_{3/2},3s_{1/2})_{1/2}$	7.701	3	7.714	0.07		
81	$(2p_{1/2})-(2p_{1/2},2p_{3/2},3s_{1/2})_{1/2}$	7.704	5	7.720	0.08		7.704
82	$(2p_{3/2})-(2p_{3/2},2p_{3/2},3s_{1/2})_{5/2}$	7.712	5	7.728	0.04	7.712	
83	$(2s_{1/2})-(2s_{1/2},2p_{3/2},3s_{1/2})_{3/2}$	7.788	4	7.803	0.12		

[a]The designation is (lower level, upper level: hole state, excited state) *J*, where hole state is the list of the missing $n=2$ electrons, excited state is the excited electron, and *J* is the total angular momentum.

[b]The calculated positions of the transitions from $2s$ hole states have been shifted to shorter wavelengths by 0.007 Å with respect to the $2p$ hole states.

[c]Hutcheon, Cooke, Key, Lewis, and Bromage (Ref. 7).

[d]Gordon, Hobby, and Peacock (Ref. 8).

[e]Blended with stronger Br XXVIII transitions.

TABLE VI. Transitions in O-like Br XXVIII.

Key	Transition[a]	Pres. Meas. λ	Relative Intensity	Pres. Calc. λ	*gf*	Prev. Meas. λ[b]
1	$(2p_{1/2},2p_{3/2})_2-(2p_{1/2},2p_{1/2},2p_{3/2},4d_{3/2})_2$	5.186	1	5.187	0.20	
2	$(2p_{1/2},2p_{3/2})_2-(2p_{1/2},2p_{1/2},2p_{3/2},4d_{3/2})_3$	5.190	1	5.189	0.54	
3	$(2p_{3/2},2p_{3/2})_2-(2p_{1/2},2p_{3/2},2p_{3/2},4d_{3/2})_2$			5.190	0.39	
4	$(2p_{3/2},2p_{3/2})_0-(2p_{1/2},2p_{3/2},2p_{3/2},4d_{3/2})_1$			5.190	0.28	
5	$(2p_{3/2},2p_{3/2})_2-(2p_{1/2},2p_{3/2},2p_{3/2},4d_{3/2})_3$			5.193	0.37	
6	$(2p_{3/2},2p_{3/2})_2-(2p_{1/2},2p_{3/2},2p_{3/2},4d_{3/2})_3$	5.210	1	5.217	0.24	
7	$(2p_{1/2},2p_{3/2})_1-(2p_{1/2},2p_{3/2},2p_{3/2},4d_{5/2})_2$	5.250	1	5.247	0.19	5.251
8	$(2p_{1/2},2p_{3/2})_2-(2p_{1/2},2p_{3/2},2p_{3/2},4d_{5/2})_3$	5.278	1	5.275	0.31	
9	$(2p_{3/2},2p_{3/2})_2-(2p_{3/2},2p_{3/2},2p_{3/2},4d_{5/2})_3$	5.299	1	5.302	3.37	5.292
10	$(2p_{1/2},2p_{1/2})_0-(2p_{1/2},2p_{1/2},2p_{1/2},4d_{5/2})_1$			5.305	0.51	
11	$(2p_{3/2},2p_{3/2})_2-(2p_{3/2},2p_{3/2},2p_{3/2},4d_{5/2})_2$					
12	$(2p_{1/2},2p_{3/2})_1-(2p_{1/2},2p_{3/2},2p_{3/2},4d_{5/2})_2$			5.311	0.48	
13	$(2p_{1/2},2p_{3/2})_2-(2p_{1/2},2p_{3/2},2p_{3/2},4d_{5/2})_3$	5.307	4	5.311	0.75	5.305
14	$(2p_{1/2},2p_{3/2})_2-(2p_{1/2},2p_{3/2},2p_{3/2},4d_{5/2})_2$	5.318	1	5.312	0.47	5.325
15	$(2p_{3/2},2p_{3/2})_0-(2p_{3/2},2p_{3/2},2p_{3/2},4d_{5/2})_1$	5.401	2	5.347	0.24	5.400
16	$(2p_{1/2},2p_{3/2})_2-(2s_{1/2},2p_{1/2},2p_{3/2},3p_{3/2})_3$	6.331	1	6.332	0.23	
17	$(2p_{1/2},2p_{3/2})_2-(2s_{1/2},2p_{1/2},2p_{3/2},3p_{1/2})_2$	6.374	c	6.374	0.12	
18	$(2p_{1/2},2p_{1/2})_0-(2s_{1/2},2p_{1/2},2p_{1/2},3p_{1/2})_1$	6.382	1	6.386	0.31	
19	$(2p_{3/2},2p_{3/2})_2-(2s_{1/2},2p_{3/2},2p_{3/2},3p_{3/2})_3$	6.408	3	6.410	0.27	

TABLE VI. (*Continued*).

Key	Transition[a]	Pres. Meas. λ	Relative Intensity	Pres. Calc. λ	*gf*	Prev. Meas. λ[b]
20	$(2p_{1/2},2p_{3/2})_2-(2s_{1/2},2p_{1/2},2p_{3/2},3p_{3/2})_1$			6.411	0.27	
21	$(2p_{1/2},2p_{3/2})_2-(2s_{1/2},2p_{1/2},2p_{3/2},3p_{3/2})_3$	6.423	1	6.422	0.25	
22	$(2p_{1/2},2p_{3/2})_2-(2s_{1/2},2p_{1/2},2p_{3/2},3p_{3/2})_2$	6.429	1	6.427	0.44	
23	$(2p_{1/2},2p_{3/2})_2-(2s_{1/2},2p_{1/2},2p_{3/2},3p_{1/2})_2$			6.435	0.11	
24	$(2p_{3/2},2p_{3/2})_2-(2s_{1/2},2p_{3/2},2p_{3/2},3p_{1/2})_2$	6.440	1	6.440	0.33	
25	$(2p_{3/2},2p_{3/2})_0-(2s_{1/2},2p_{1/2},2p_{3/2},3p_{3/2})_1$			6.440	0.11	
26	$(2p_{3/2},2p_{3/2})_2-(2s_{1/2},2p_{3/2},2p_{3/2},3p_{1/2})_1$	6.449	1	6.449	0.21	
27	$(2p_{3/2},2p_{3/2})_0-(2s_{1/2},2p_{3/2},2p_{3/2},3p_{3/2})_1$			6.455	0.21	
28	$(2p_{3/2},2p_{3/2})_2-(2s_{1/2},2p_{3/2},2p_{3/2},3p_{3/2})_2$	6.461	1	6.463	0.23	
29	$(2p_{1/2},2p_{3/2})_2-(2s_{1/2},2p_{1/2},2p_{3/2},3p_{1/2})_3$	6.475	2	6.473	0.43	
30	$(2p_{1/2},2p_{3/2})_1-(2s_{1/2},2p_{1/2},2p_{3/2},3p_{1/2})_2$			6.473	0.15	
31	$(2p_{3/2},2p_{3/2})_2-(2s_{1/2},2p_{3/2},2p_{3/2},3p_{3/2})_1$	6.489	1	6.491	0.13	
32	$(2p_{3/2},2p_{3/2})_2-(2s_{1/2},2p_{3/2},2p_{3/2},3p_{3/2})_3$	6.502	2	6.505	0.37	
33	$(2p_{1/2},2p_{3/2})_1-(2s_{1/2},2p_{3/2},2p_{3/2},3p_{3/2})_2$	6.542	c	6.539	0.20	
34	$(2p_{1/2},2p_{3/2})_1-(2p_{1/2},2p_{1/2},2p_{3/2},3d_{5/2})_1$	6.589	2	6.584	0.13	
35	$(2p_{3/2},2p_{3/2})_2-(2p_{1/2},2p_{3/2},2p_{3/2},3d_{5/2})_2$	6.622	2	6.615	0.13	
36	$(2p_{1/2},2p_{3/2})_1-(2p_{1/2},2p_{1/2},2p_{3/2},3d_{3/2})_2$	6.635	c	6.631	0.90	6.624
37	$(2p_{3/2},2p_{3/2})_2-(2p_{1/2},2p_{3/2},2p_{3/2},3d_{5/2})_3$			6.650	0.38	
38	$(2p_{1/2},2p_{3/2})_1-(2p_{1/2},2p_{1/2},2p_{3/2},3d_{3/2})_1$	6.656	1	6.658	0.79	
39	$(2p_{3/2},2p_{3/2})_2-(2p_{1/2},2p_{3/2},2p_{3/2},3d_{5/2})_1$	6.663	2	6.665	0.66	
40	$(2p_{1/2},2p_{3/2})_1-(2p_{1/2},2p_{1/2},2p_{3/2},3d_{3/2})_0$	6.668	2	6.666	0.37	
41	$(2p_{3/2},2p_{3/2})_0-(2p_{1/2},2p_{3/2},2p_{3/2},3d_{3/2})_1$	6.675	2	6.674	1.40	
42	$(2p_{1/2},2p_{3/2})_2-(2p_{1/2},2p_{1/2},2p_{3/2},3d_{3/2})_2$			6.676	1.11	
43	$(2p_{3/2},2p_{3/2})_2-(2p_{1/2},2p_{3/2},2p_{3/2},3d_{3/2})_2$	6.679	3	6.681	1.56	6.675
44	$(2p_{3/2},2p_{3/2})_2-(2p_{1/2},2p_{3/2},2p_{3/2},3d_{3/2})_1$			6.681	0.52	
45	$(2p_{1/2},2p_{3/2})_2-(2p_{1/2},2p_{1/2},2p_{3/2},3d_{3/2})_3$			6.681	2.38	
46	$(2p_{1/2},2p_{3/2})_2-(2p_{1/2},2p_{1/2},2p_{3/2},3d_{5/2})_3$	6.684	2	6.684	1.28	
47	$(2p_{3/2},2p_{3/2})_2-(2p_{1/2},2p_{3/2},2p_{3/2},3d_{3/2})_3$	6.690	5	6.692	3.37	
48	$(2s_{1/2},2p_{3/2})_1-(2s_{1/2},2p_{1/2},2p_{3/2},3d_{5/2})_2$	6.692	c	6.692	1.30	
49	$(2p_{1/2},2p_{3/2})_2-(2p_{1/2},2p_{1/2},2p_{3/2},3d_{3/2})_1$	6.702	2	6.703	0.11	
50	$(2p_{3/2},2p_{3/2})_2-(2p_{1/2},2p_{3/2},2p_{3/2},3d_{5/2})_2$	6.706	2	6.707	0.72	
51	$(2p_{3/2},2p_{3/2})_2-(2p_{1/2},2p_{3/2},2p_{3/2},3d_{5/2})_1$	6.711	1	6.714	0.16	
52	$(2s_{1/2},2p_{3/2})_2-(2s_{1/2},2p_{1/2},2p_{3/2},3d_{5/2})_3$	6.720	c	6.725	1.74	
53	$(2s_{1/2},2p_{3/2})_2-(2s_{1/2},2p_{1/2},2p_{3/2},3d_{3/2})_1$	6.720	c	6.725	0.89	
54	$(2s_{1/2},2p_{3/2})_2-(2s_{1/2},2p_{1/2},2p_{3/2},3d_{3/2})_2$	6.720	c	6.726	2.02	
55	$(2s_{1/2},2p_{3/2})_1-(2s_{1/2},2p_{1/2},2p_{1/2},3d_{3/2})_2$			6.733	2.16	
56	$(2p_{3/2},2p_{3/2})_2-(2p_{1/2},2p_{3/2},2p_{3/2},3d_{3/2})_3$	6.739	3	6.743	0.35	
57	$(2p_{3/2},2p_{3/2})_2-(2p_{1/2},2p_{3/2},2p_{3/2},3d_{5/2})_3$	6.749	2	6.752	0.30	
58	$(2p_{3/2},2p_{3/2})_2-(2p_{1/2},2p_{3/2},2p_{3/2},3d_{3/2})_2$	6.753	2	6.757	0.32	
59	$(2p_{1/2},2p_{3/2})_1-(2p_{1/2},2p_{3/2},2p_{3/2},3d_{3/2})_1$	6.760	1	6.763	0.22	
60	$(2p_{1/2},2p_{3/2})_1-(2p_{1/2},2p_{3/2},2p_{3/2},3d_{5/2})_2$	6.776	c	6.780	1.35	
61	$(2p_{1/2},2p_{3/2})_2-(2p_{1/2},2p_{3/2},2p_{3/2},3d_{5/2})_2$			6.827	0.58	6.834
62	$(2p_{1/2},2p_{3/2})_2-(2p_{1/2},2p_{3/2},2p_{3/2},3d_{5/2})_3$	6.826	c	6.827	1.56	
63	$(2p_{1/2},2p_{3/2})_1-(2p_{1/2},2p_{3/2},2p_{3/2},3d_{5/2})_2$			6.833	0.28	
64	$(2p_{1/2},2p_{3/2})_1-(2p_{1/2},2p_{3/2},2p_{3/2},3d_{5/2})_1$			6.833	0.16	
65	$(2p_{1/2},2p_{1/2})_0-(2p_{1/2},2p_{1/2},2p_{3/2},3d_{5/2})_1$	6.835	4	6.840	2.26	
66	$(2p_{1/2},2p_{3/2})_2-(2p_{1/2},2p_{3/2},2p_{3/2},3d_{3/2})_2$	6.843	1	6.844	0.75	
67	$(2p_{1/2},2p_{3/2})_1-(2p_{1/2},2p_{3/2},2p_{3/2},3d_{3/2})_2$	6.850	2	6.849	0.62	
68	$(2p_{1/2},2p_{3/2})_1-(2p_{1/2},2p_{3/2},2p_{3/2},3d_{3/2})_1$			6.850	0.55	
69	$(2p_{3/2},2p_{3/2})_2-(2p_{3/2},2p_{3/2},2p_{3/2},3d_{5/2})_3$	6.853	5	6.852	2.50	
70	$(2p_{1/2},2p_{3/2})_1-(2p_{1/2},2p_{3/2},2p_{3/2},3d_{5/2})_0$			6.856	0.21	
71	$(2p_{1/2},2p_{3/2})_2-(2p_{1/2},2p_{3/2},2p_{3/2},3d_{5/2})_3$	6.864	3	6.865	2.12	6.866
72	$(2p_{1/2},2p_{3/2})_1-(2p_{1/2},2p_{3/2},2p_{3/2},3d_{5/2})_2$	6.876	4	6.877	1.04	6.877
73	$(2p_{1/2},2p_{3/2})_2-(2p_{1/2},2p_{3/2},2p_{3/2},3d_{5/2})_2$	6.881	2	6.881	0.83	
74	$(2p_{1/2},2p_{3/2})_2-(2p_{1/2},2p_{3/2},2p_{3/2},3d_{5/2})_1$			6.881	0.64	
75	$(2p_{1/2},2p_{3/2})_1-(2p_{1/2},2p_{3/2},2p_{3/2},3d_{5/2})_1$			6.884	0.29	
76	$(2p_{3/2},2p_{3/2})_2-(2p_{3/2},2p_{3/2},2p_{3/2},3d_{5/2})_2$	6.886	5	6.887	0.69	
77	$(2p_{1/2},2p_{3/2})_2-(2p_{1/2},2p_{3/2},2p_{3/2},3d_{3/2})_2$			6.898	0.12	
78	$(2p_{3/2},2p_{3/2})_2-(2p_{3/2},2p_{3/2},2p_{3/2},3d_{3/2})_1$	6.909	1	6.911	0.12	

TABLE VI. (*Continued*).

Key	Transition[a]	Pres. Meas. Relative Intensity λ	Pres. Calc. λ	Pres. Calc. *gf*	Prev. Meas. λ[b]
79	$(2p_{3/2},2p_{3/2})_0-(2p_{3/2},2p_{3/2},2p_{3/2},3d_{5/2})_1$	6.928 2	6.928	0.77	
80	$(2p_{1/2},2p_{3/2})_1-(2p_{1/2},2p_{1/2},2p_{3/2},3s_{1/2})_2$	7.078 c	7.079	0.11	
81	$(2p_{1/2},2p_{3/2})_2-(2p_{1/2},2p_{1/2},2p_{3/2},3s_{1/2})_2$	7.125 1	7.131	0.10	7.123
82	$(2p_{3/2},2p_{3/2})_2-(2p_{1/2},2p_{3/2},2p_{3/2},3s_{1/2})_3$	7.132 c	7.132	0.20	
83	$(2p_{3/2},2p_{3/2})_2-(2p_{1/2},2p_{3/2},2p_{3/2},3s_{1/2})_2$	7.181 2	7.181	0.10	
84	$(2p_{3/2},2p_{3/2})_2-(2p_{3/2},2p_{3/2},2p_{3/2},3s_{1/2})_1$	7.336 1	7.334	0.17	
85	$(2p_{1/2},2p_{3/2})_1-(2p_{1/2},2p_{3/2},2p_{3/2},3s_{1/2})_1$		7.362	0.14	
86	$(2p_{1/2},2p_{1/2})_0-(2p_{1/2},2p_{1/2},2p_{3/2},3s_{1/2})_1$		7.363	0.11	
87	$(2p_{1/2},2p_{3/2})_2-(2p_{1/2},2p_{3/2},2p_{3/2},3s_{1/2})_2$	7.368 3	7.365	0.27	7.370

[a]The designation is (lower level, upper level: hole state, excited state) J, where hole state is the list of the missing $n=2$ electrons, excited state is the excited $n=3$ or $n=4$ electron, and J is the total angular momentum.
[b]Gordon, Hobby, and Peacock (Ref. 8).
[c]Blended with Br XXVII or Br XXVI transitions.

our measured wavelengths agree with the calculated wavelengths to within several mÅ.

The O-like transitions are somewhat weaker than the F-like and Ne-like transitions in the high-irradiation spectrum, and several of the O-like transitions are blended with stronger F-like or Ne-like transitions. In addition, there are a number of cases in which strong O-like transitions have nearly the same wavelength and overlap in the spectrum. The large number of overlaps results from the relatively large number of levels (five) within the ground configuration of the O-like ion. In contrast, the ground configuration of the F-like and Ne-like ions have only two levels and one level, respectively, and chance overlaps are less likely to occur.

V. CONCLUSIONS

The spectra of Br XXIV–XXVIII were produced using the microdot technique. Spatially resolved, single-shot spectra were recorded for laser irradiation intensities from 3×10^{13} to 4×10^{14} W/cm^2. Based on the variation of the spectral line intensities with the laser irradiation intensity and with the distance from the target, it was possible to distinguish the Mg-like and Na-like satellite transitions from the transitions in more highly charged ions. The spectral resolution obtained using the microdot technique is a significant improvement over previous work, and the present work greatly expands the number of identified transitions in Br XXIV, XXV, XXVII, and XXVIII.

ACKNOWLEDGMENTS

The authors wish to express their thanks to K. Reed for his contribution to the *ab initio* calculations and to A. Hazi and R. Fortner for useful discussions. Work performed under the auspices of the U.S. Department of Energy by Lawrence Livermore National Laboratory under Contract No. W-7405-Eng-48.

*Permanent address: E. O. Hulburt Center for Space Research, Naval Research Laboratory, Washington, D.C., 20375

[1]D. L. Matthews, P. L. Hagelstein, M. D. Rosen, M. J. Eckart, N. M. Ceglio, A. U. Hazi, M. Medecki, B. J. MacGowan, J. E. Trebes, B. L. Whitten, E. M. Campbell, C. W. Hatcher, A. M. Hawryluk, R. L. Kauffman, L. D. Pleasance, G. Rambach, J. H. Scofield, G. Stone, and T. A. Weaver, Phys. Rev. Lett. **54**, 110 (1985).
[2]M. D. Rosen, P. L. Hagelstein, D. L. Matthews, E. M. Campbell, A. U. Hazi, B. L. Whitten, B. MacGowan, R. E. Turner, R. W. Lee, G. Charatis, Gar. E. Busch, C. L. Shepard, P. D. Rockett, and R. R. Johnson, Phys. Rev. Lett. **54**, 106 (1985).
[3]J. P. Apruzese, J. Davis, M. Blaha, P. C. Kepple, and V. L. Jacobs, Phys. Rev. Lett. **55**, 1877 (1985).
[4]B. L. Whitten, A. U. Hazi, M. H. Chen, and P. L. Hagelstein, Phys. Rev. A **33**, 2171 (1986).
[5]P. G. Burkhalter, D. J. Nagel, and R. D. Cowan, Phys. Rev. A **11**, 782 (1975).
[6]V. A. Boiko, A. Ya. Faenov, and S. A. Pikuz, J. Quant. Spectrosc. Radiat. Transfer **19**, 11 (1978).
[7]R. J. Hutcheon, L. Cooke, M. H. Key, C. L. S. Lewis, and G. E. Bromage, Phys. Scr. **21**, 89 (1980).
[8]H. Gordon, M. G. Hobby, and N. J. Peacock, J. Phys. B **13**, 1985 (1980).
[9]H. Gordon, M. G. Hobby, N. J. Peacock, and R. D. Cowan, J. Phys. B **12**, 881 (1979).
[10]J. Bailey, R. E. Stewart, J. D. Kilkenny, R. S. Walling, T. Phillips, R. J. Fortner, and R. W. Lee, J. Phys. B (to be published).
[11]M. J. Herbst, P. G. Burkhalter, J. Grun, R. R. Whitlock, and M. Fink, Rev. Sci. Instrum. **53**, 1418 (1982).
[12]P. G. Burkhalter, M. J. Herbst, D. Duston, J. Gardner, M. Emery, R. R. Whitlock, J. Grun, J. P. Apruzese, and J. Davis, Phys. Fluids **26**, 3650 (1983).
[13]U. I. Safronova, Phys. Scr. **23**, 241 (1981).
[14]J. Scofield (unpublished).